Mechanical study of sintered aromatic polyesters as revealed by microindentation measurements

A. FLORES AND F. J. BALTÁ CALLEJA

Instituto de Estructura de la Materia, CSIC, Serrano 119, Madrid 28006, Spain

H. R. KRICHELDORF

Institut für Technische und Makromolekulare Chemie, Bundesstrasse 45, D-20146 Hamburg, Germany

Abstract

The micromechanical properties of a new series of sintered aromatic polyesters have been studied. Load-displacement curves obtained from a depth-sensing indentation instrument are used to evaluate the viscoelastic-plastic properties of these aromatic polyesters. The depths investigated lay within the micron scale. Hardness values derived from this technique are compared with those obtained using a microindentation tester. The influence of particle morphology and unit cell symmetry on the mechanical properties of these materials has been investigated. The possible variation of hardness with the sintering pressure applied on the sample preparation has been examined. The viscoelastoplastic properties of these new aromatic polyesters are discussed in the light of those previously reported on related aromatic homopolymers.

1. Introduction

Poly(4-hydroxybenzoate) (PHB) and poly(2-hydroxy-6-naphthoate) (PHN) homopolymers have been the focus of much scientific research during the past twenty years [1-9]. Their synthesis [1-5], crystal structure [1,2,4-8] and thermal transitions [1,2,4-7,9] have been investigated. In a preceding paper, we have studied the mechanical properties of cold sintered PHB and PHN homopolymers using the microhardness technique [10]. These homopolymers possess mechanical properties in compression comparable to those of some metals such as aluminium or silver [11]. In a recent work we reported on the synthesis of a new series of aromatic polyesters derived from diphenols or diphenyldiols and dicarboxylic or biphenyl dicarboxylic acids [12]. Their morphology, crystal structure and thermal transitions were reported in reference [12]. Aromatic rigid polyesters are potential candidates to possess good mechanical properties in compression. The aim of this letter is to report about the mechanical properties of these new aromatic polyesters using the microhardness and ultramicrohardness techniques.

Indentation with a sharp indenter, involving deformation on a very small scale, is one of the simplest ways to measure the mechanical properties of a material surface. The microhardness technique has become a widely accepted and easy method to measure the mechanical properties of polymers [13, 14]. This technique is based on the optical measurement of the residual image of the indented area. Hardness is sensitive to structural changes in the amorphous or crystalline phase of polymers [13, 14]. On the other hand, hardness is related to macroscopic mechanical properties such as the yield stress [13, 14]. Hence, it is an adequate technique to measure the plastic properties of the material. However, the information about the viscoelastic recovery of the material during the removal of the load is lost when measuring with the imaging technique.

The ultramicrohardness technique records the load-displacement data during an indentation experiment [15-24]. This technique has the advantage that, not only the viscoelastic properties of the material can be determined, but that small loads can also be applied, opening up, in addition, the possibility of studying the mechanical properties of thin films. Ultramicrohardness technique has become gradually widespread in the study of the plastic and elastic properties of metals and ceramics [15-21]. However, its application to polymers is still in a very initial stage [22-24]. Indeed, some studies on the ultramicrohardness of poly(ethylene terephthalate) (PET) [23], poly(isobutadiene) rubber

(PIB), poly(ether-ether ketone) (PEEK), poly(methyl methacrylate) (PMMA), Nylon-6 [24] and poly(propylene) (PP) [22] have been recently reported.

In the present paper, a combination of the micro and the ultramicrohardness technique is used to comparatively evaluate the viscoelastic-plastic properties of the above series of aromatic polyesters. The values of hardness determined using the depth-sensing technique are thus compared with those obtained using the imaging method.

2. Experimental details

2.1. Materials

Fig.1 shows the repeating units of the new aromatic polyesters investigated (numbers 1-5). The chemical repeat unit of PHB and PHN homopolymers are also included in figure 1 (numbers 6 and 7 respectively). All samples were available in powder form. Polyesters number 1 to 5 were polycondensated at 400°C using the 'HCl method'. Polyester 5 was polycondensated from naphthalene-2,6-dicarbonylchloride (20 mmol) and 2,6-naphthalenediol (20 mmol) which were weighed into a 500 ml three-necked flask containing Marlotherm-S (200 ml). The reaction vessel was placed into a metal bath preheated to 150 °C and the temperature was rapidly raised to 400 °C. The liberated HCl was removed with a slow stream of nitrogen. Polyester 5 began to crystallize after 20-30 minutes. The reaction mixture was cooled after 6 hours, the polyester was isolated by filtration, intensively washed with hot acetone and finally dried out at 120 °C in vacuo. A yield of 77% was obtained. Polyesters 1-4 were prepared in a similar manner with yields in the range of 83-97%. Details of the synthesis of polyesters 1-3 are reported on a previous paper [12].

1 mm thick plates were obtained from all samples after sintering the respective powders at room temperature for 10 minutes under a pressure of 0.19 and 0.70 GPa. In addition, polyester 1 was compression moulded under a pressure of 0.011 GPa at 335 °C for 10 minutes.

2.2. Techniques

Microindentation experiments were carried out using a **Leitz microhardness tester**. A Vickers square based indenter was used. The contact area was obtained by measuring the

residual image of the projection of the indented area [13]. The hardness value, H, was derived using the following equation:

$$H = k\frac{F}{d^2} \qquad (1)$$

where F is the applied force, d is the diagonal length of the indentation and k is a geometric constant equal to 1.854. The applied forces employed were varied between 0.10 and 0.49 N. A 6 seconds holding time of the indenter was chosen to minimise creep.

Ultra-microindentation experiments were performed using a **Shimadzu dynamic hardness tester**. A Vickers indenter was used with a semiangle between opposite faces of the pyramid α=68°. Cycles of the type load-hold-unload were obtained with a peak load of 0.15 N. The maximum load applied was reached by increasing the load at a constant rate (see fig. 2). The time consumed in the loading cycle was 11 s. The peak load was held thereafter for 6 seconds. The unloading cycle was performed at the same constant rate as the loading cycle. The values of the maximum load applied, time employed in the loading/unloading cycle and holding time at maximum load were selected so as to be comparable with those used in a microindentation experiment. Typical values for the maximum penetration depth (h_{max} in fig. 2) and the final penetration depth (h_f) for the samples investigated range between 8.5-10 μm and 6-7 μm respectively. As h_{max} > 2 μm, hardness values obtained from micro and ultramicroindentation experiments should be comparable [25]. Force - displacement data were transferred to a computer program for their analysis. Values of hardness, H, and elastic modulus, E, were derived from the unloading curves using the procedure of Doerner and Nix [21]:

$$H = \sin 68° \frac{P_{max}}{k' h_p^2} \qquad (2)$$

$$E = \sqrt{\frac{\pi}{k'}} \frac{dP/dh}{2\,hp} \quad (1-\nu^2) \qquad (3)$$

where k' is a geometrical constant equal to 24.5, P_{max} is the maximum load applied, h_p is the plastic depth, $^{dP}/_{dh}$ is the unloading slope at peak load and ν is the Poisson ratio of the material. The plastic depth is calculated by extrapolating to zero load a tangent to the unloading curve at maximum load (see fig. 2). Poisson's ratio was taken to be 0.4 for all samples [26].

3. Results and discussion

3.1. Influence of morphology and grain size.

Table 1 collects the hardness values experimentally determined using the microhardness tester (imaging method), $H_{imaging}$, and the ultramicroindenter (depth-sensing method), H_{depth}, and the elastic modulus values for the series of polymers with different chemical composition and sintered at the highest pressure (0.70 GPa). $H_{imaging}$ of polyesters PHB and PHN with different crystal morphologies are taken from reference [10]. The referred hardness values for PHB and PHN correspond to samples sintered at the same pressure (0.70 GPa) as the new synthesized polyesters (samples 1-5). The hardness value obtained for each of the new materials investigated seemed to be insensitive to the pressure applied in the sample preparation. Therefore, we have not included in table 1 the hardness value for a 0.19 GPa sintering pressure. On the contrary, values of the hardness of PHB and PHN were shown to be dependent on the sintering pressure applied as previously reported [10].

Although all polyesters (1-7) were obtained in powder form, there are some differences on the powder grain size of polyesters 1-5 with respect to that of polyesters 6,7. From all the investigated PHB and PHN samples, polyester 6 in its slab-like crystal morphology presents the finest grain size and, at the same time, the smallest H variation with the sintering pressure applied (see ref. 10). This sample shows, when examined under the optical microscope, globular conglomerates whose average size lies in the range 200-500 μm. On the other hand, the average size of the conglomerates of polyesters 1-5 lies in the range 50-200 μm. This difference in size could explain the observed insensitivity of the hardness value with the sintering pressure for polyesters 1-5. The intergranular packing would be favoured in the smaller polyester particles so that it does not seem to improve with pressure in the range investigated. It would also be reasonable to expect hardness values for polyesters 1-5 enhanced with respect to those

of polyesters 6,7. However, table 1 shows higher H for polyesters 6,7 suggesting other factors contributing to H. Hardness is known to strongly depend on crystallinity [14] but in our previous investigation [10] we pointed out the fact that there was no correlation between the degree of crystallinity and the microhardness values of the sintered materials. In this case, particle morphology may have a determinant role. Polyesters 1-5 show irregular shaped particles and no whiskers were present. It is possible that the different particle morphology between polyesters 1-5 and 6,7 would give rise to different hardness values. However, we attempt to give an alternative explanation.

3.2. Influence of unit cell symmetry

PHB and PHN present an orthorhombic unit cell at room temperature which is transformed into a pseudohexagonal chain packing above a first order transition at temperatures 300°-350°C [1, 4, 7]. This transition implies flip motions and librations of the phenylene groups [27]. On the other hand, polyesters 1-5 present a unit cell at room temperature which is already closer to an hexagonal packing than the unit cell corresponding to polyesters 6-7, implying an enhanced segmental mobility. Therefore, the easier yield behaviour in polyesters 1-5 showing an enhanced segmental mobility gives rise to lower H values than in the case of polyesters 6 and 7, which present a more compact packing of the molecules in the unit cell. One measure for the type of chain packing within the crystals is given by the angle γ defined by the intersection of the unit cell diagonals ($\gamma = 120°$ if the cell is hexagonal). Table 1 also collects the values of the γ angle of the unit cell measured at room temperature for all the polyesters under study except for polyester 5 where no data are available (see ref. 6,7,12). Figure 3 shows the variation of the hardness value as a function of the γ angle. It is worth pointing out that hardness values for $\gamma>106°$ correspond to samples with finely divided powders, thus, hardness values in the range $106°<\gamma<120°$ are probably enhanced with respect to those for $\gamma\leq106°$. As a whole, the hardness value shows a clear tendency to diminish as γ tends towards 120°. This means that as the chain packing relaxes towards an hexagonal symmetry, the molecules will exhibit an increased segmental mobility leading to smaller H values. Nuclear magnetic resonance measurements of polyester 4 with deuterated terephthalic acid indicate significant motion in the crystalline phase in support of these findings [28].

It is worth mentioning that the compression moulded sample of polyester 1 reveals a hardness value when measured with the imaging technique of 191 MPa which is notably much higher than that obtained in the sintered sample. This large difference could be related to the limited molecular diffusion between particles in the sintered sample. Previous investigations have shown that the sintering process at room temperature is not sufficient to induce a molecular diffusion similar to that occurring in the molten state [10].

3.3. Viscoelastic properties

Figure 4 shows the plot of H versus E derived from depth-sensing data. The hardness values obtained using the imaging method are also included. $H_{imaging}$ is generally higher than H_{depth} except for PHB (fibrous whisker morphology) and PHN (whisker morphology) where the H error is so large that $H_{imaging}$ and H_{depth} are coincident. This big uncertainty in H is a consequence of a rather coarse powder which leads to inhomogenities along the sample. The fact that $H_{imaging}$ is clearly higher than H_{depth} in polyesters 5, 6 (whisker morphology) and 7 (slab-like morphology) could be explained as a viscoelastic recovery of the indentation diagonal upon the removal of the load. $H_{imaging}$ in polyesters 1-4 is only slightly higher than H_{depth} and this difference may be considered within the error limits. A first order regression fit to the H_{depth}- E values gives two different slopes, H/E=0.038 and 0.056. Data fitted to the slope H/E=0.056 show a higher deviation of the $H_{imaging}$ values with respect to the H_{depth} values in accordance to an enhanced viscoelastic behaviour. The values of H/E can be directly related to the ratio between the elastic and plastic components of the total penetration depth at maximum load, h_e/h_p (see fig. 2). Figure 5 illustrates the plot of h_e/h_p values of all polyesters versus H_{depth}/E. As the elastic component decreases with respect to the plastic contribution to the total depth, the material approaches H/E=0, which represents the case of ideal plasticity. One can show that with a combination of equations (2) and (3), h_e/h_p is directly proportional to H/E where the constant of proportionality is equal to $(1\text{-}0.4^2)\frac{\sqrt{24.5\pi}}{2\sin 68°}$, which is the slope of the straight line in figure 5.

4. Conclusions

–The hardness values measured at room temperature of cold sintered aromatic polyesters derived from diphenols/diphenyldiols and dicarboxylic/biphenyl dicarboxylic acids (samples 1-5) are lower than the values previously reported for PHB and PHN.

–Microhardness is shown to be dependent on the γ angle between the diagonals of the orthorhombic crystal lattice and on the morphology of the polymer particles.

–In case of polyester 1, compression moulding at high temperature gives rise to higher mechanical properties than cold sintering. Similar results were reported for polyesters PHB and PHN.

–It turns out that the hardness value of polymers 1-5 are independent on the sintering pressure. This finding has been ascribed to the smaller grain size of these samples in contrast to polyesters 6, 7.

–Hardness values evaluated using the imaging technique are higher than those derived from the depth-sensing data probably due to the viscoelastic recovery of the diagonal indentation. The difference between these two values tends to increase with the increasing value of H/E.

Acknowledgements

The authors are grateful to DGICYT, Spain (Grant PB94-0049) for the support of this investigation.

References

1. H. R. KRICHELDORF, G. SCHWARZ, *Polymer*, **31** (1990) 481.
2. H. R. KRICHELDORF, G. SCHWARZ, F. RUHSER, *Macromolecules*, **24** (1991) 3485.
3. H. R. KRICHELDORF, G. SCHWARZ, *Polymer*, **25** (1984) 520.
4. G. SCHWARZ, H. R. KRICHELDORF, *Macromolecules*, **24** (1991) 2829.
5. A. MÜHLEBACH, J. LYERLA, J. ECONOMY, *Macromolecules*, **22** (1989) 3741.
6. S. HANNA, A. H. WINDLE, *Polymer*, **33** (1992) 2825.
7. S. HANNA, A. H. WINDLE, *Polym. Comm.*, **29** (1988) 236.
8. G. LIESER, *J. Polym. Sci.: Polym. Phys. Ed.*, **21** (1983) 1611.

9. J. ECONOMY, W. VOLKSEN, C. VINEY, R. GEISS, R. SIEMENS, T. KARIS, *Macromolecules*, **21** (1988) 2777.
10. A. FLORES, F. ANIA, F. J. BALTÁ CALLEJA, H. R. KRICHELDORF, *J. Mater. Sci. Lett.*, **14** (1995) 1571.
11. F. J. BALTÁ CALLEJA, S. FAKIROV, *Trends Polym. Sci.*, **5** (1997) 246.
12. H. R. KRICHELDORF, O. STRUVE, G. SCHWARZ, *Polymer*, **37** (1996) 4311.
13. F. J. BALTÁ CALLEJA, *Adv. Poly. Sci.*, **66** (1985) 117.
14. F. J. BALTÁ CALLEJA, *Trends Polym. Sci.*, **2** (1994) 419.
15. J. L. LOUBET, J. M. GEORGES, O. MARCHESINI, G. MEILLE, *J. Tribology*, **106** (1984) 43.
16. V. RAMAN, R. BERRICHE, *J. Mater. Res.*, 7 (1992) 627.
17. P. J. BLAU, J. R. KEISER, R. L. JACKSON, *Mater. Charac.*, **30** (1993) 287.
18. E. VANCOILLE, J. P CELIS, J. R. ROOS, *Thin Solid Films*, **224** (1993) 168.
19. G. M. PHARR, W. C. OLIVER, F. R. BROTZEN, *J. Mater. Res.*, 7 (1992) 613.
20. W. C. OLIVER, G. M. PHARR, *J. Mater. Res.*, 7 (1992) 1564.
21. M. F. DOERNER, W. D. NIX, *J. Mater. Res.*, **1** (1986) 601.
22. J. GUBICZA, A. JUHÁSZ, P. TASNÁDI, P. ARATÓ, G. VÖRÖS, *J. Mater. Sci.*, **31** (1996) 3109.
23. R. H. ION, H. M. POLLOCK, C. ROQUES-CARMES, *J. Mater. Sci.*, **25** (1990) 1444.
24. B. J. BRISCOE, K. S. SEBASTIAN, S. K. SINHA, *Phil. Mag. A*, **74** (1996) 1159.
25. A. FLORES, F. J. BALTÁ CALLEJA, Proceedings of the E. P. S., Surfaces and Interfaces in Polymers and Composites (Lausanne, 1997).
26. A. W. BIRLEY, B. HAWORTH, J. BATCHELOR, "Physics of Plastics" (Oxford University Press, New York,1992).
27. T. THOMSEN, H. G. ZACHMANN, H. R. KRICHELDORF, *J. Macromol. Sci. Phys. (B)*, **30** (1991) 87.
28. F. v. STEIN, W. GRONSKI, J. BLACKWELL, S. N. CHVALUN, H. R. KRICHELDORF, *Macromolecules* (1998) (in press).

Legend to Figures

Figure 1 Chemical repeating units of the aromatic polyesters investigated.

Figure 2 Variation of penetration depth of the indenter as a function of applied load during a loading-hold-unloading cycle.

Figure 3 Variation of indentation hardness as a function of angle between diagonals of crystal unit cell.

Figure 4 Plot of H vs. E for the studied samples.

Figure 5 Plot of the ratio between the elastic and plastic contribution to the total penetration depth at maximum load versus the H/E ratio.

Repeating unit	Processing	Morphology	γ (°)	$H_{imaging}$ (MPa)	H_{depth} (MPa)	E (GPa)
1	Sintering	Irregular particles	110	119	115	3.1
1	Compression moulded at 0.01 GPa	–	110	191	–	–
2	Sintering	Irregular particles	120	92	90	2.2
3	Sintering	Irregular particles	108	109	102	2.6
4	Sintering	Irregular particles	108	112	104	2.6
5	Sintering	–	–	120	78	1.3
6	Sintering	Whiskers	106	150	128	3.5
6	Sintering	Fibrous whiskers	106	197	218	4.3
6	Sintering	Slab-like crystals	106	163	–	–
7	Sintering	Whiskers	105	172	192	2.9
7	Sintering	Slab-like crystals	105	149	115	2.1

TABLE I Indentation hardness and elastic modulus of aromatic polyesters with different morphologies and chemical structure (see fig.1).

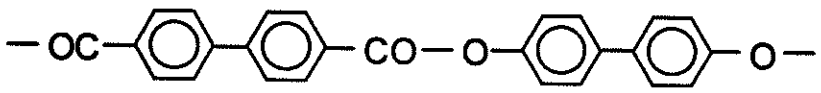

1

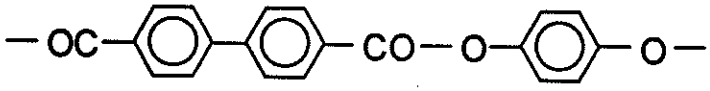

2

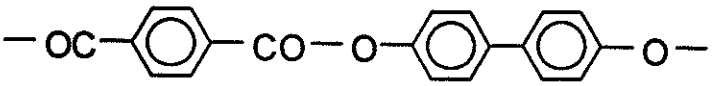

3

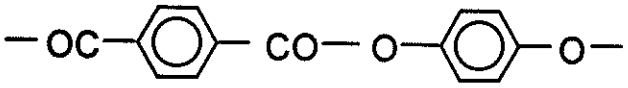

4

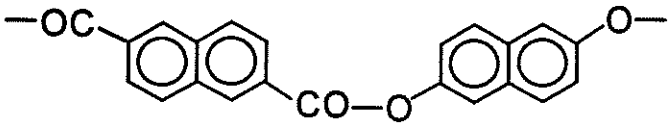

5

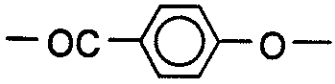

6

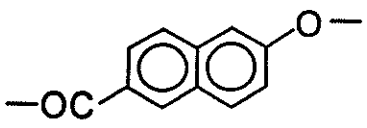

7

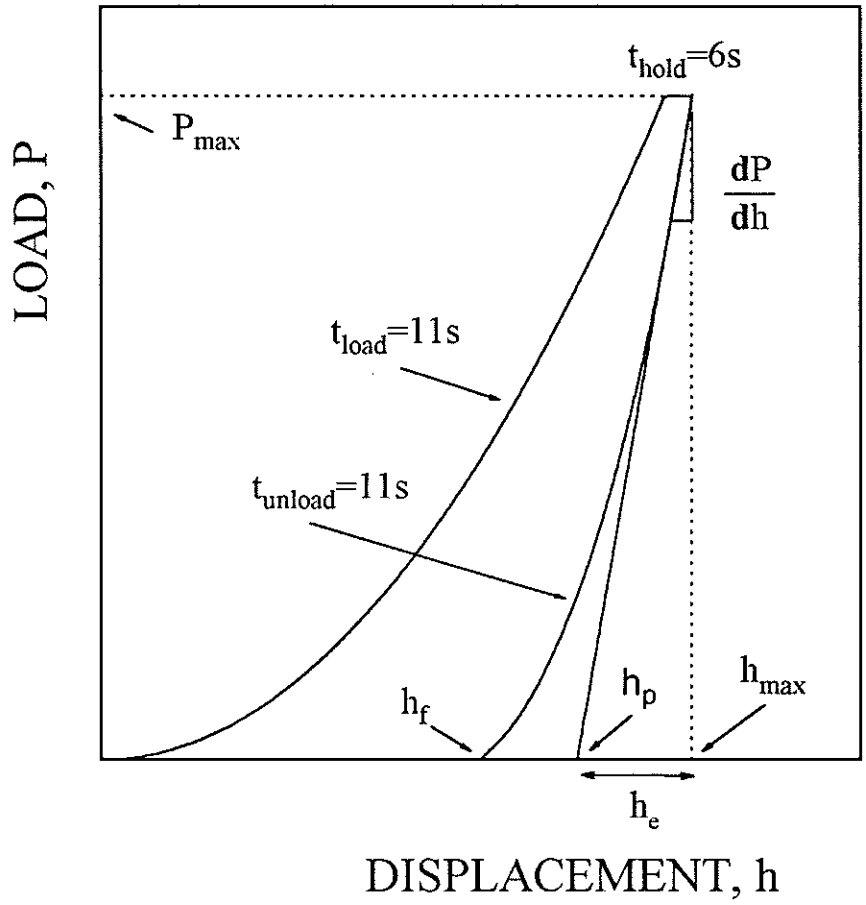
LOAD, P
t_{hold}=6s
P_{max}
dP
dh
t_{load}=11s
t_{unload}=11s
h_f
h_p
h_{max}
h_e
DISPLACEMENT, h

Figure 2

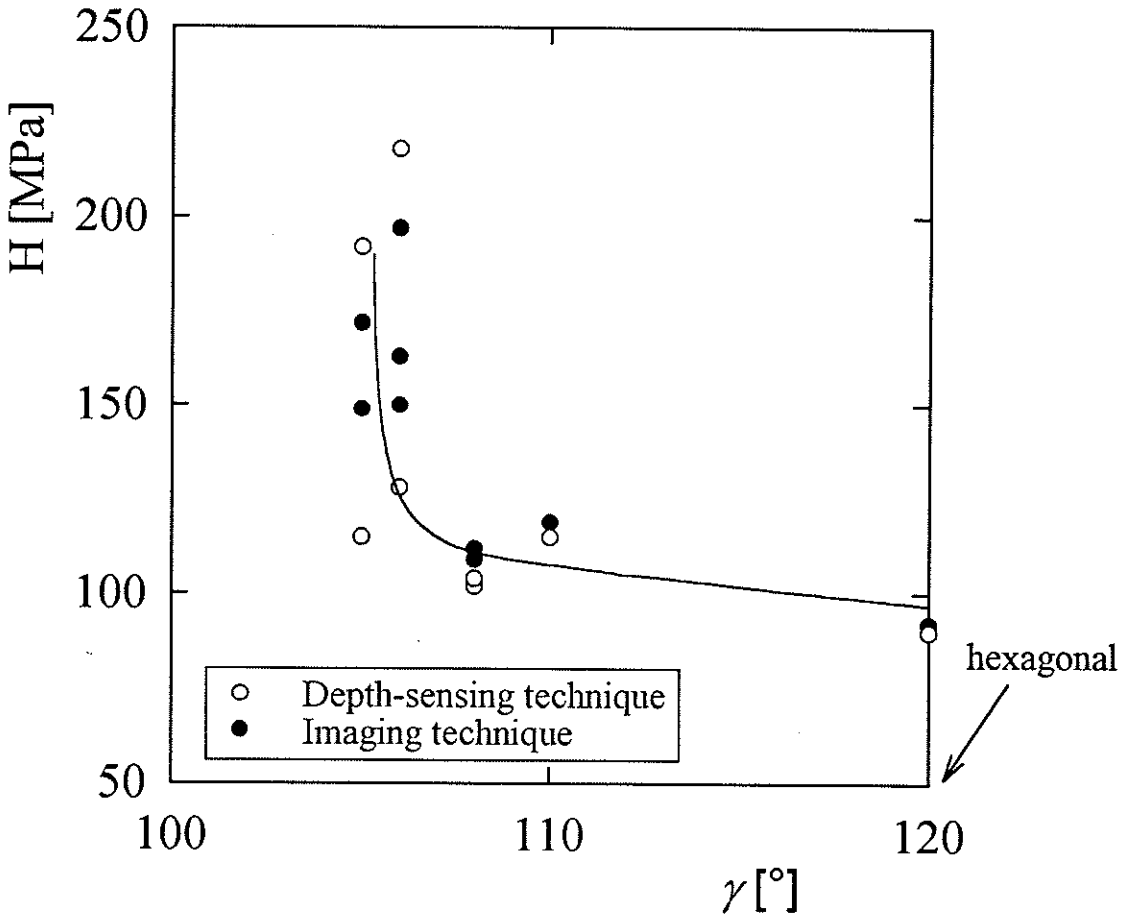
250
200
150
100
50
H [MPa]
100
110
120
γ [°]
Depth-sensing technique
Imaging technique
hexagonal

Figure 5

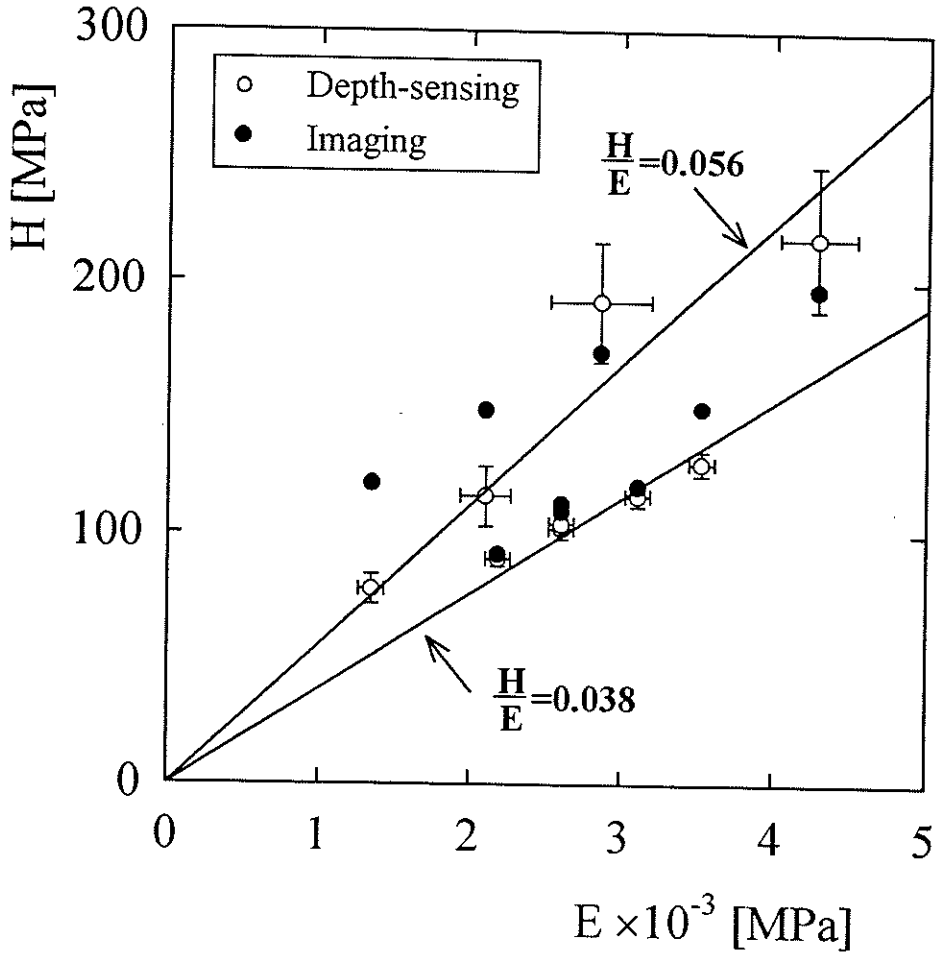
300
200
100
0
H [MPa]
Depth-sensing
Imaging
H/E=0.056
H/E=0.038
0
1
2
3
4
5
E ×10-3 [MPa]

Figure 4

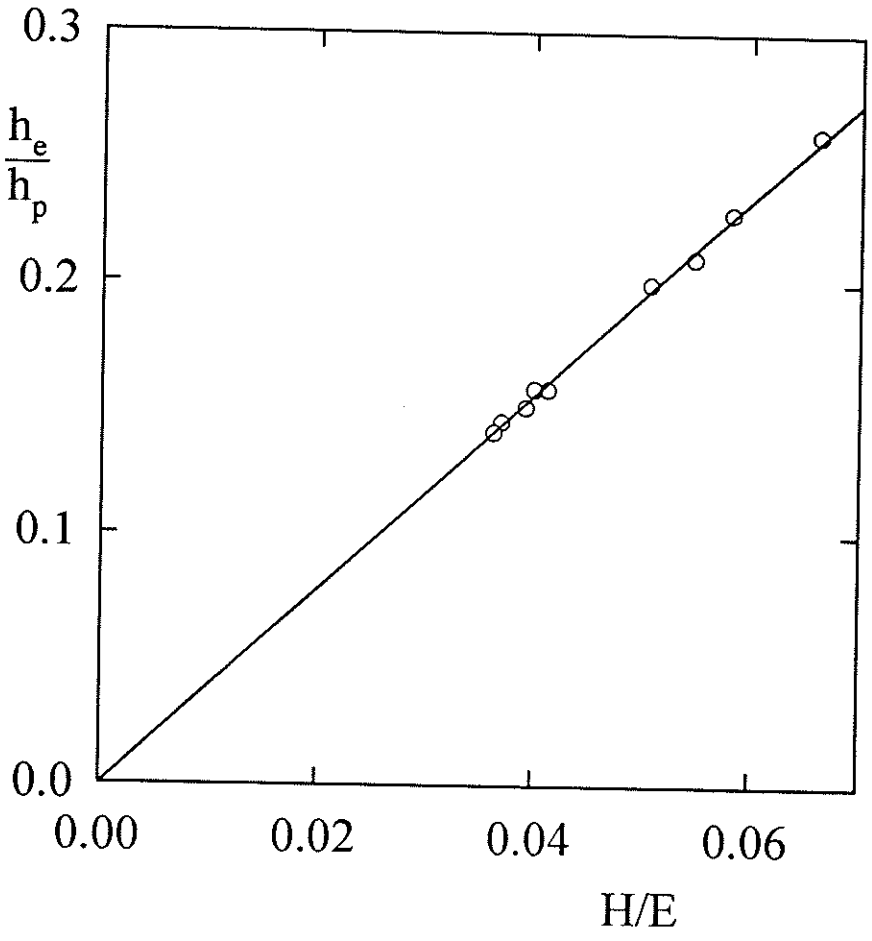

Figure 6